Differences in Cross-Link Chemistry between Rigid and Flexible Dithiol Molecules Revealed by Optical Studies of CdTe Quantum Dots

R. Koole,*,† B. Luigjes,† M. Tachiya,‡ R. Pool,† T. J. H. Vlugt,† C. de Mello Donegá,† A. Meijerink,† and D. Vanmaekelbergh†

Debye Institute, Condensed Matter and Interfaces, Utrecht University, P.O. Box 80 000, 3508 TA Utrecht, The Netherlands, and National Institute of Advanced Industrial Science and Technology, Tsukuba, Ibaraki 305-8565, Japan

Received: March 27, 2007; In Final Form: May 18, 2007

The cross-link chemistry of CdTe quantum dots (QDs) in solution is studied for different types of aliphatic (flexible) and aromatic (rigid) dithiol linker molecules. A remarkable difference in the cross-linking efficiency is observed: the rigid dithiols are shown to form aggregates at much lower concentrations. Qualitative and quantitative information on the formation of aggregates is obtained from cryogenic transmission electron microscopy (cryo-TEM) images and photoluminescence decay measurements. The luminescence decay curves are analyzed with a model for energy transfer to neighboring QDs in aggregates. The analysis shows that the cross-linking efficiency is 4 times higher for the rigid dithiols than for the flexible dithiols. The difference is attributed to the formation of loops for the flexible dithiols by attaching with both thiol groups to the same nanocrystal surface (preventing cross-linking), whereas the rigid aromatic dithiols cannot form loops and the second thiol group is oriented away from the surface (enabling cross-linking). The difference in conformation between flexible and rigid dithiols is confirmed by studies on the red-shift in the optical absorption spectra due to capping exchange of amines by monothiols or dithiols and by molecular simulations.

Introduction

To control the distance-dependent interactions between two quantum dots (QDs), both lithographic and epitaxial growth techniques have been successfully applied. The opto-electronic properties of such a double-QD structure have been studied in detail, and it was shown that a precise tuning of the electronic coupling can be achieved by a careful design of the structure.[1−3] Alternatively, semiconductor QDs can be prepared by wet chemistry resulting in colloidal dispersions of semiconductor nanocrystals with well-defined shape and size. It is a challenge in current nanoscience to use these nanocrystals as building blocks for the assembly of new superstructures such as QD molecules and superlattices and to analyze the collective properties, which depend on the interactions between the individual QDs. Superlattices can be made by self-assembly of colloidal QDs on a substrate, and by choosing the right conditions, long-range ordering can be obtained, even with binary structures.[4] However, to study the interactions between neighboring QDs by optical spectroscopy, superlattices of colloidal QDs on a substrate are less suitable due to scattering processes and the relatively low signal from a monolayer of nanocrystals. Well-defined smaller aggregates of only a few QDs in solution (QD-molecules) are more promising to study the optical properties of interacting QDs. It is therefore important to have a high degree of control over the chemical cross-linkage of QDs in dispersion. Dithiol molecules have been used extensively to cross-link nanocrystals (i.e., Au nanocrystals), but the exact conformation of these cross-linkers on a nanocrystal surface is still under debate.[5,6] There is an interesting connection of this topic to the field of self-assembled monolayers (SAMS), where the conformation of dithiol molecules on a gold substrate is still subject of extensive discussions.[7] The understanding of the conformation of these dithiols on a substrate or nanocrystal is of great importance, because thiol end-functionalized molecules hold great promise for the field of molecular electronics.[6,8−10]

Here, we report the effect of the rigidity of different dithiol cross-linker molecules on the cross-link chemistry of CdTe QDs. Information on the cross-linking is obtained from cryogenic transmission electron microscopy (cryo-TEM) studies and the optical properties of the resulting QD-aggregates. Both aliphatic (flexible) and aromatic (rigid) dithiol molecules were used to cross-link green-emitting CdTe QDs (gQDs) in solution. The three types of investigated rigid molecules are the same as Dadosh et al. used for single-molecule conductance measurements: 4,4′-biphenyldithiol (BPD), bis-(4-mercaptophenyl)-ether (BPE), and 1,4-benzenedimethanethiol (BdMT) (see the insets in Figure 3).[6] Triggered by their results on how the conjugation of the molecule determines the conductance, we aimed at a control over the degree of electronic coupling between CdTe QDs by using these three differently conjugated rigid cross-linker molecules. In addition, we used the flexible aliphatic molecules hexanedithiol (HdT) and nonanedithiol (NdT) to cross-link the QDs (see the insets in Figure 2).

Interestingly, we found that the aromatic rigid molecules (BPD, BPE, BdMT) act as very efficient linkers, at least 4 times more efficient than the flexible aliphatic cross-linkers (HdT, NdT). The distinct cross-link properties of the different dithiol molecules reported and explained here are of great interest for the field of molecular electronics, in which these molecules are also extensively investigated. Surprisingly, no reduction of the

* Corresponding author. E-mail: r.koole@phys.uu.nl. Phone: +31-30-2532207. Fax: +31-30-2532403.
† Utrecht University.
‡ National Institute of Advanced Industrial Science and Technology.

10.1021/jp072407x CCC: $37.00 © 2007 American Chemical Society
Published on Web 07/07/2007

optical gap is observed in the gQD-aggregates when BPD, BPE, or BdMT (rigid) is used as a cross-linker, in contrast to QDs cross-linked by HdT and NdT (flexible).[11] However, a detailed study on the influence of monothiols on the optical properties of CdTe and CdSe QDs shows that even a small amount of monothiols bound to the QD surface can cause a reduction of the optical gap. This implies that the previous interpretation of the reduced optical gap in CdTe aggregates originating from electronic coupling is not correct, as will be discussed at the end of this article.[11]

Experimental Section

Green (Ø 3.4 ± 0.5 nm), yellow (Ø 3.8 nm), and red (Ø 5.1 ± 0.7 nm) emitting CdTe QDs were synthesized in a mixture of $Cd(Me)_2$ (ARC Technologies), trioctylphosphine (TOP, Fluka), tellurium powder (Heraeus), and dodecylamine (DDA, Aldrich), as reported earlier.[11,12] Particle sizes were determined by the analysis of TEM images. The synthesis of the CdSe QDs used in this report is described in detail elsewhere.[13] The QDs were capped with allylamine (AA, Aldrich) by a ligand exchange; 1 mL of crude QD product was mixed with 1 mL AA and heated for 4 h at 50 °C. The concentration of AA-capped QDs was determined by the absorbance value at the first absorption peak and the molar extinction coefficient, which was derived from the QD size (TEM) and the size-dependent formula obtained by Yu et al.[14] An accurately weighed amount of HdT (hexanedithiol), NdT (nonanedithiol), BPE (bis-(4-mercaptophenyl)-ether), BdMT (1,4-benzenedimethanethiol) (Aldrich), and BPD (4,4′-biphenyldithiol, T.C.I. Europe) was dispersed in toluene and diluted to the various desired concentrations. Solutions of different linker/QD ratios were prepared by adding a well-defined and constant quantity of AA-capped QDs to 0.5 mL toluene, in which the cross-linker was dissolved at varying concentrations. After 3 days, the dispersions were diluted to 5 mL with toluene to perform the optical measurements. In a similar way, the samples with varying monothiol/QD ratios were prepared, starting with a stock solution of PT (propanethiol), HT (hexanethiol), NT (nonanethiol), BT (benzenethiol), and PET (2-phenylethanethiol) (all purchased from Aldrich). All experiments were performed at room temperature, under nitrogen atmosphere. The excitation wavelength for all emission and photoluminescence decay measurements was 406 nm. We refer to the Supporting Information and a previous publication for further experimental and instrumental details.[11]

Results and Discussion

Cryo-TEM. QD-aggregates at various linker/QD ratios were synthesized by accurately varying the concentration of the cross-linker molecule in a dispersion of CdTe QDs (see the Experimental Section). The QDs were capped with the short ligand AA, to avoid sterical hindrance during cross-linkage and to enable an as small as possible interdot distance. To study the size of the aggregates obtained by the cross-linkage of the CdTe QDs at different linker/QD ratios, we performed cryo-TEM on two series of QD-aggregates, one using a flexible cross-linker (HdT) and the other using a rigid cross-linker (BPD). By counting between 100 and 500 QDs per sample, the composition of the aggregates (i.e., single QDs and number of QDs/aggregate) was analyzed (see Figure 1, cryo-TEM images can be found in the Supporting Information). In both series, the fraction of single QDs decreases with increasing linker/QD ratio, whereas the fraction of aggregates increases. It should be noted that even without a cross-linker molecule, dimers (two QDs/aggregate) and a few trimers are present. Importantly, the results show a clear difference between the cross-link efficiency, which is higher for the rigid BPD molecules. For example, to reduce the fraction of single QDs to 0.2, about 10 times more HdT is needed compared to BPD. Furthermore, the concentration of dimers in the BPD series clearly reaches a maximum at a linker/QD ratio between 0.25:1 and 0.5:1, which can be expected if each cross-linker binds to two QDs. For the flexible HdT molecules, the maximum concentration of dimers is reached at much higher concentrations (8:1). Clearly, BPD cross-links the QDs significantly more efficient than HdT.

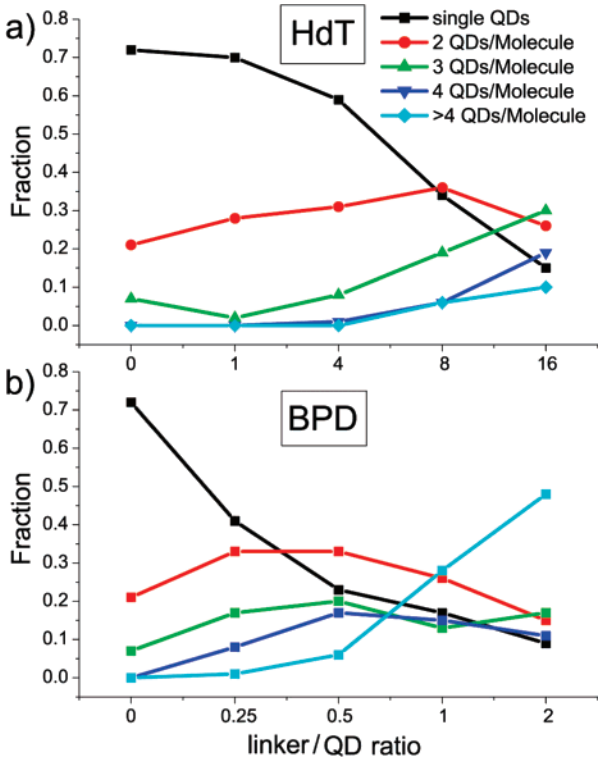

Figure 1. Fraction of QDs present as single QDs or as QD-molecules of different sizes as a function of the linker/QD ratio, using HdT (a) or BPD (b) as the cross-linker molecule. Note the difference in scale for the *x*-axis in panels a and b.

Absorption and Emission Spectroscopy. Identification of QDs and QD-aggregates from cryo-TEM images is not trivial and may not be representative for the aggregation of the ensemble of QDs in solution. To obtain further information on the aggregate size and the interaction between QDs in the aggregates, we used optical spectroscopy: the absorption and emission spectra, and photoluminescence decay curves were measured. Absorption and emission spectra were measured for a series of linker/QD ratios for each of the five different cross-linker molecules (Figures 2 and 3). The difference in cross-link efficiency between HdT and BPD observed in cryo-TEM also appears in the absorption measurements, because scattering (nonzero absorption at $\lambda > 650$ nm) of the dispersions of both HdT and NdT cross-linked QDs consistently occurred at much higher linker/QD ratios (between 16:1 and 20:1) than for the BPD, BPE, or BdMT cross-linked QDs (between 3:1 and 4:1). Individual QDs are too small to scatter light, but large clusters of QDs (in the size regime of tens of nanometers) can scatter light, which appears in the absorption spectrum as a background of decreasing transmission toward shorter wavelength. The scattering is most clearly observed in the wavelength region where the QDs in the solution do not absorb light (>650 nm).[11] Because both HdT and NdT appeared to cross-link the QDs

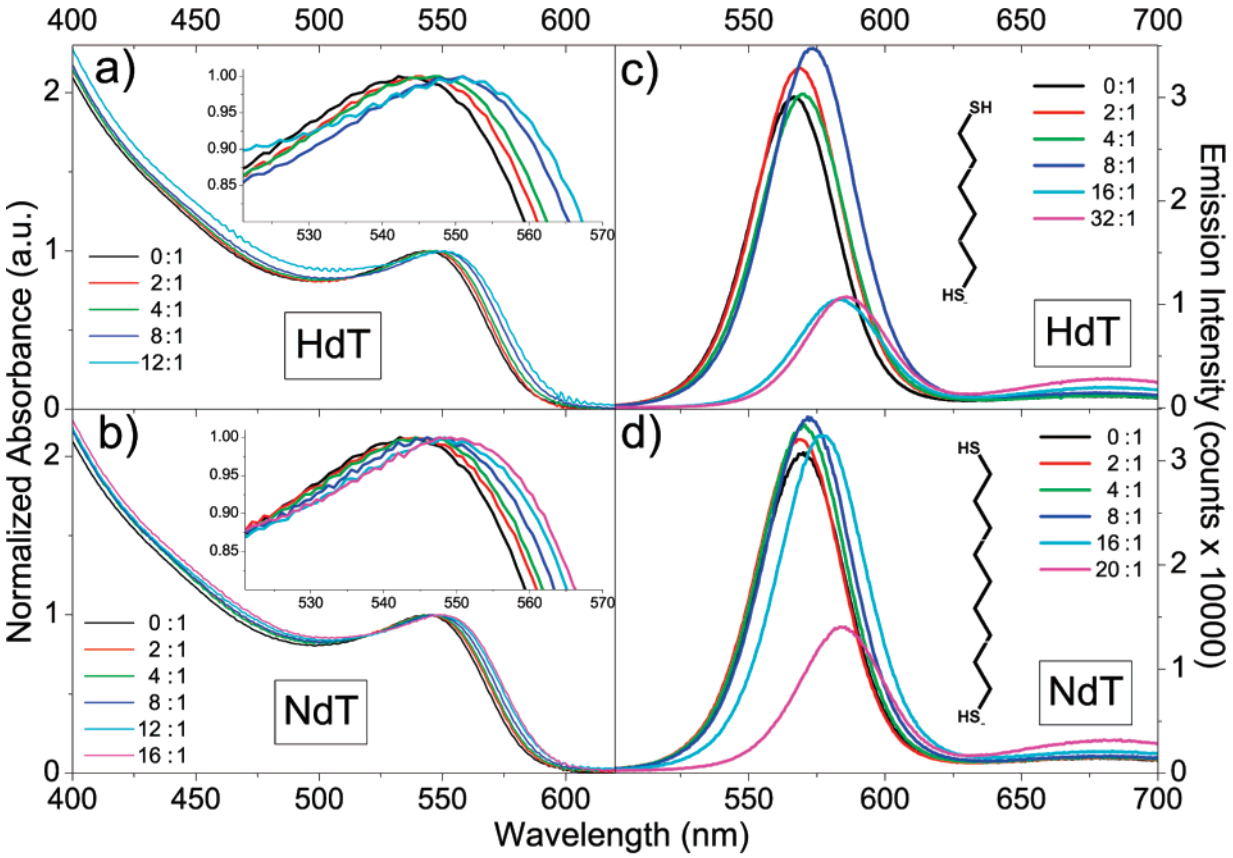

Figure 2. Absorption (a and b) and emission (c and d) spectra of gQD-molecules at different linker/QD ratios, using HdT or NdT as the cross-linker molecule. Insets show a magnification of the first absorption peak. Absorption spectra are normalized at the first absorption peak ($\lambda \approx 550$ nm).

less efficiently than the other three molecules (BPD, BPE, BdMT), a different range of linker/QD ratios was chosen for the two groups of cross-linkers.

For the cross-linkers HdT and NdT, a behavior similar to that reported earlier is observed.[11] Up to a HdT/QD ratio of 12:1 (16:1 for NdT), a gradual and similar red-shift up to 35 meV is seen in both absorption and emission spectra, without a decrease in the emission intensity (Figure 2). The red-shift in absorption and emission were previously attributed to electronic coupling between neighboring QDs, resulting in a decrease of the optical gap. However, an alternative explanation for this observation will be discussed at the end of this article. At higher linker/QD ratios, a decrease in emission intensity is observed, accompanied by an increase in the defect-related emission ($\lambda > 650$ nm). These are signatures of (multistep) exciton energy transfer, which is confirmed by lifetime measurements (vide infra). Especially in the larger clusters, energy transfer between neighboring QDs results in trapping of the exciton on a QD with a defect, thus increasing the intensity of the defect-related emission at the cost of the exciton emission intensity (Figure 2, parts c and d).

When the QDs are cross-linked by BPD, BPE, or BdMT, the system behaves differently. Already at low concentrations of these rigid cross-linker molecules (linker/QD ratio between 0:1 and 2:1), the emission spectra (Figure 3d−f) show a gradual shift and decrease in emission intensity as the concentration of cross-linker increases. In addition, the defect-related emission increases as a function of cross-linker concentration. For this concentration regime no red-shift in the absorption spectra is observed (Figure 3a−c). At higher cross-linker concentrations, scattering hampers the analysis of the absorption spectrum, and therefore a red-shift cannot be resolved. The gradual red-shift and decrease in emission intensity can be explained by exciton energy transfer, which was also seen for the CdTe aggregates cross-linked by flexible molecules (Figure 2). Finally, it should be noted that the changes in emission spectra due to energy transfer are similar for all three rigid linker molecules (Figure 3d−f). This indicates that the differences in molecular structure between the three cross-linkers do not significantly influence the energy transfer process. The fact that red-shifts are only observed in the emission spectra and not in the absorption spectra shows that electronic coupling is not important. This will be discussed in more detail at the end of this article.

As was mentioned above, both cryo-TEM and optical absorption measurements suggest that cross-linkage by the rigid dithiol molecules is more efficient than by flexible molecules. To provide additional evidence and to quantify the differences in cross-linking by the flexible and rigid dithiol molecules, we performed time-resolved photoluminescence measurements of CdTe gQDs at various linker/QD ratios with flexible and rigid cross-linkers. Two examples of the luminescence decay curves for CdTe gQDs cross-linked by HdT (flexible) and BPD (rigid) are shown in Figure 4 (the other decay curves can be found in the Supporting Information). Without cross-linker (0:1), the gQDs display a nearly monoexponential luminescence decay, indicating the high quality of the QDs and enabling a quantitative analysis. On the other hand, the gQD-aggregates cross-linked by HdT (32:1) and BPD (4:1 and 8:1) show a multiexponential decay, which is ascribed to exciton energy transfer. The decay curves were measured at an emission wavelength of 535 nm, which is at the far blue side of the emission spectrum of the gQDs (Figure 2c). QDs emitting at this wavelength will act as donors, and can transfer their energy to neighboring QDs that have a smaller band gap (acceptors). The fast initial decay

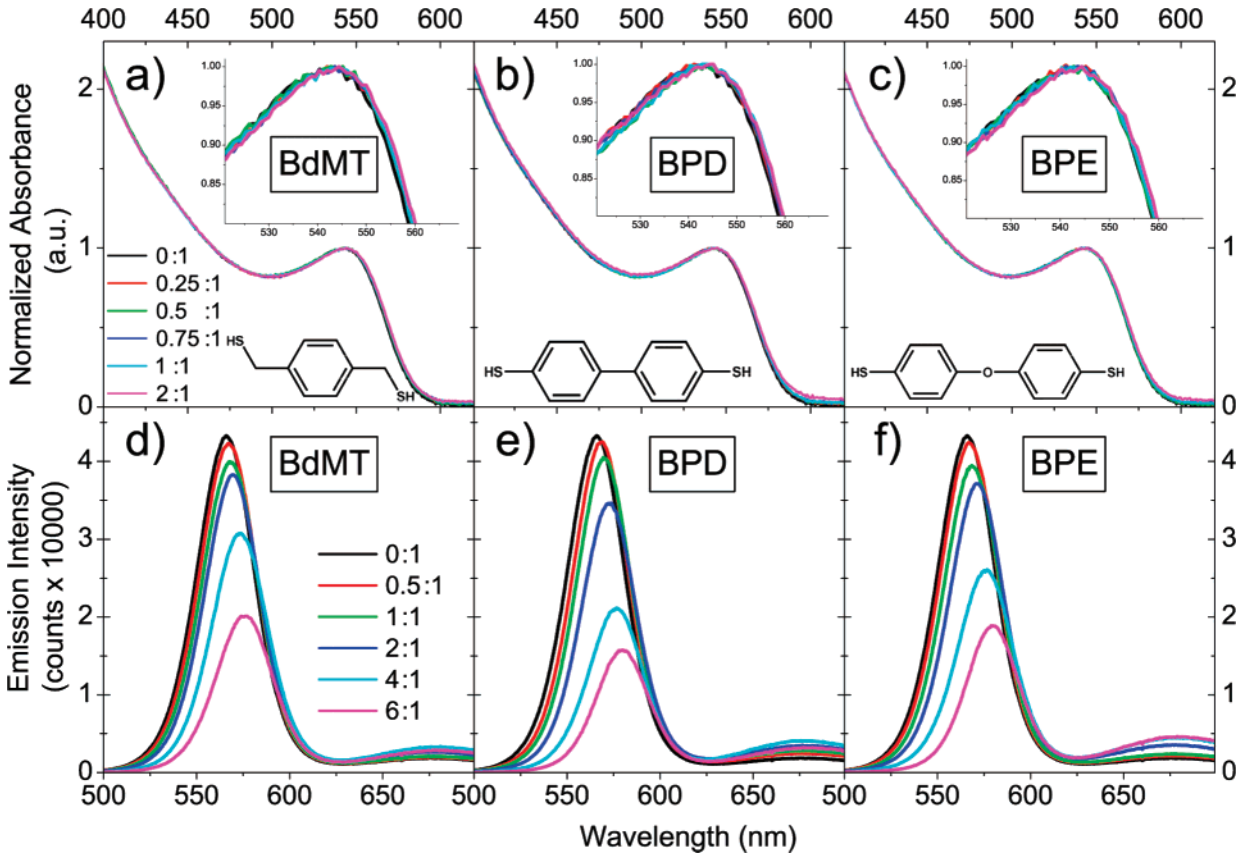

Figure 3. Absorption (a−c) and emission (d−f) spectra of gQD-molecules at different linker/QD ratios, using BPD, BPE, or BdMT as the cross-linker molecule. Insets show a magnification of the first absorption peak. Absorption spectra are normalized at the first absorption peak ($\lambda \approx 550$ nm).

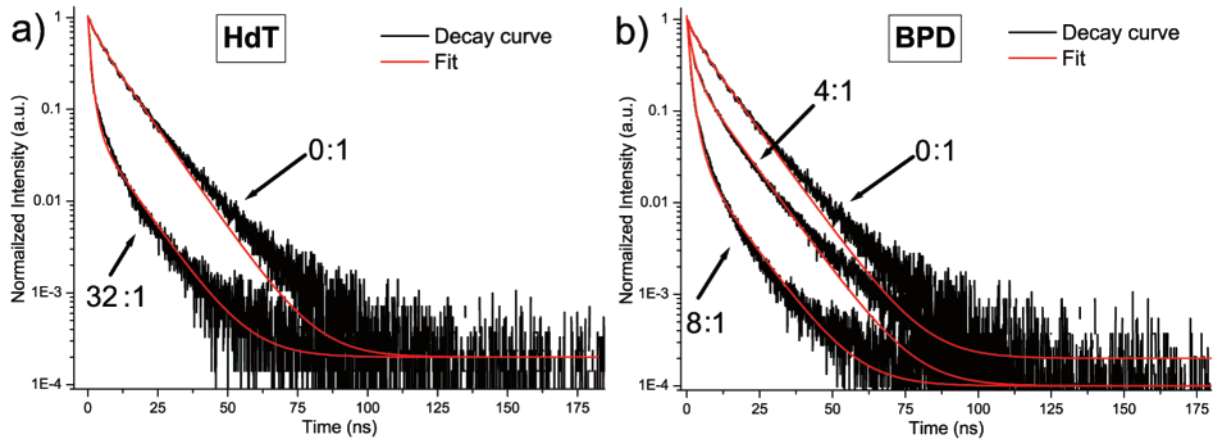

Figure 4. Decay curves of gQDs cross-linked with (a) HdT and (b) BPD at different linker/QD ratios. Red curves show the results of fitting the curves with eq 1. (Excitation wavelength = 406 nm, emission wavelength = 535 nm.)

in the decay curves measured for QDs in the presence of cross-linkers is attributed to QDs that are part of an aggregate. The total decay rate (Γ_{tot}) of QDs in an aggregate is the sum of the radiative decay rate (Γ_{rad}, typically 0.1 ns^{-1}) and the energy transfer rate (Γ_{ET}), which is between 20 and 0.5 ns^{-1} (transfer time between 50 ps and 2 ns) in QD solids.[15−18] The subsequent slow decay in these curves is attributed to single QDs that are not part of an aggregate, which display a radiative decay that is similar to the QDs without cross-linker (0:1).

Photoluminescence Decay Measurements. To obtain quantitative information about the cross-link efficiency of the different molecules, we fitted the decay curves to the following equation, the derivation of which is given in the Supporting Information:

$$I(t) = I_0 \exp[(-\Gamma_{rad}t) - n(1 - e^{(-\Gamma_{ET}t)})] + y_0 \qquad (1)$$

Here I_0 is a normalization constant and y_0 is a constant that corrects for the background signal. The variable n is the average number of acceptor QDs cross-linked to a donor QD, and Γ_{ET} is defined as the energy transfer rate to one neighboring QD. This formula was developed earlier for a different system of emitting probes with neighboring quenchers.[19] In the present case, the model describes the luminescence decay kinetics of

TABLE 1: Overview of the Values for Γ_{ET}, *n*, and *f* at Different Linker/QD Ratios

	gQDs with HdT			rQDs with HdT				gQDs with BPD		
HdT/QD	Γ_{ET} (ns^{-1})	*n*	*f*	Γ_{ET} (ns^{-1})	*n*	*f*	BPD/QD	Γ_{ET} (ns^{-1})	*n*	*f*
8:1				0.44	0.7	0.08	2:1	0.30	1.0	0.40
16:1	0.59	1.1	0.06	0.42	2.0	0.12	4:1	0.34	1.4	0.30
32:1	0.40	2.8	0.08	0.30	3.5	0.10	6:1	0.31	2.7	0.37
							8:1	0.28	3.5	0.36
							10:1	0.24	3.8	0.32
							12:1	0.25	3.9	0.28

the dispersions of gQDs in the presence of cross-linkers, where the number of QDs cross-linked to another QD obeys a Poisson distribution. To connect *n* to a cross-link efficiency of the different molecules, we define *z* as the molar ratio of cross-linkers to QDs (i.e., linker/QD = 16:1 gives $z = 16$) and *f* as the fraction of cross-linkers that have a QD attached on both ends. Assuming that all linker molecules attach to the QDs, the variables *z* and *f* can be used to calculate *m*, which is the average number of linker molecules attached to a QD:

$$m = \frac{z}{\left(1 - \frac{1}{2}f\right)} \tag{2}$$

The average number *n* of acceptor QDs cross-linked to a donor QD is the product of *m* and *f* and can thus be expressed in terms of *z* and *f*:

$$n = mf = \frac{zf}{\left(1 - \frac{1}{2}f\right)} \tag{3}$$

By fitting the decay curves using eq 1, the value for *n* could be extracted. Because the molar ratio of cross-linkers to QDs is known (*z*), the fraction of cross-linkers that has a QD attached on both ends (*f*) can be calculated for that particular system, which directly relates to the cross-link efficiency.

We fitted the decay curves by fixing the radiative rate (Γ_{rad}) to 0.1 ns^{-1} and setting y_0 to a value equal to the background measured. The other parameters (*n* and Γ_{ET}) were fitted, and examples of the resulting fits are represented by red solid lines in Figure 4. As can be seen, the model describes the decay curves well. We found that Γ_{rad} varies between 0.09 and 0.1 ns^{-1} for the different linker/QD ratios if this parameter is allowed to vary as well, close to the value that is found when the decay curve for the sample without cross-linkers (0:1) is fitted by a single-exponential fit. We fixed Γ_{rad} at 0.1 ns^{-1} because this gives the best fits for the decay curves with cross-linkers, from which the parameters *n* and Γ_{ET} were extracted. However, this value yields a lower quality fit for the decay curve without cross-linkers (0:1), which explains the deviation of the fit in the long time regime (>50 ns). We fitted all decay curves of gQD cross-linked by HdT and BPD at different linker/QD ratios. In addition, we fitted the decay curves of red-emitting CdTe QDs (rQDs) cross-linked by HdT. This was to obtain additional information about the cross-link properties of flexible molecules and to see if the cross-link behavior is independent of the nanocrystal size. The decay curves and fits to eq 1 that are not shown in Figure 4 can be found in the Supporting Information. An overview of the values for *n* and Γ_{ET} that were extracted from the fitting curves and the values of *f* are given in Table 1.

From Table 1 it can be seen that the average value of *f* is about 0.08 when HdT is used as cross-linker. Therefore, it can be concluded that about 1 out of 13 HdT molecules has a QD attached on both ends ($f \approx 0.08$; $1/f \approx 13$) when used to cross-link QDs. The values of *f* for gQDs and rQDs cross-linked with HdT are approximately the same. This indicates that the cross-linking efficiency is independent of the nanocrystal size. When gQDs are cross-linked with a rigid cross-linker (BPD), the average value of *f* is 0.34, which means that 1 out of 3 BPD molecules has a QD attached at both sides. This value is over 4 times higher than that for the flexible cross-linker HdT, confirming the above observations that the rigid molecules cross-link the QDs more efficiently than flexible molecules. Furthermore, the ET rate (Γ_{ET}) was extracted from the fits. In our model, Γ_{ET} is defined as the rate at which an exciton is transferred to one neighboring QD, which is multiplied by *n* in eq 1 to obtain the total ET rate due to all neighboring acceptors. Therefore, the value extracted for Γ_{ET} from the fits should be independent of the linker/QD ratio, as is indeed the case, especially for the gQD cross-linked with BPD (0.29 ± 0.04 ns^{-1}). In the case of QDs cross-linked by HdT, there is a larger spread in the Γ_{ET} values, which we ascribe to experimental uncertainty. Note that that up to the present day, the ET rates that have been reported in the literature ($20-0.5$ ns^{-1}) were measured in QD solids, where the interdot distance and amount of neighbors is not well defined.[15−18] Here we show that the energy transfer rate from one QD in solution to another single neighboring QD at a distance of about 1 nm (the size of BPD) is ~ 0.3 ns^{-1}.

The Γ_{ET} obtained for gQDs cross-linked with HdT (≈ 0.4 ns^{-1}) seems to be higher as compared to the Γ_{ET} of gQDs cross-linked by BPD (0.3 ns^{-1}). The slower ET rate in the latter case may be due to a longer (and fixed) interparticle distance due to the rigid cross-linker but may also be due to the uncertainty resulting from the analysis. It was reported earlier that the interparticle distance between gold nanoparticles that were cross-linked by aromatic dithiols was consistent with the size of the molecule, confirming the rigidity of these dithiols.[5,6,20]

The optical analysis described above is a very sound tool to study a structural property of dithiol molecules on a nanocrystal surface. From the analysis of the decay curves (Table 1), it can be concluded that cross-linking of QDs by rigid molecules (BPD, BPE, BdMT) is at least 4 times more efficient than for the flexible molecules (HdT, NdT). To explain this difference we consider that both HdT and NdT contain a single aliphatic chain which gives the molecules a high rotational freedom around the carbon chain. We propose that flexible cross-linkers can therefore attach with both thiol groups to one single QD to form loops, whereas rigid molecules cannot. Because a significant fraction of the flexible molecules will form loops on one QD, a higher number of the flexible cross-linker molecules is needed compared to the rigid molecules to achieve a similar aggregation number. Further support for this explanation is provided by molecular simulations and optical absorption measurements for QDs in the presence of monothiols and dithiols, as explained below.

Molecular Simulations. We performed molecular simulations showing that HdT indeed forms loops on a gold nanocrystal (Figure 5a), whereas more rigid molecules do not (Figure 5b).

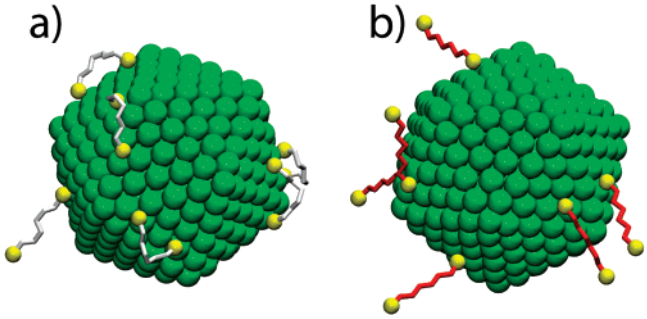

Figure 5. Snapshots from molecular simulations showing the configuration of (a) flexible hexanedithiol molecules (gray bonds) and (b) rigid hexanedithiol molecules (red bonds) on a gold nanocrystal (green), dispersed in hexane. The figure shows typical snapshots from well-equilibrated simulations. Note that, for clarity, the solvent molecules are not shown.

Although the simulations were performed on a gold nanocrystal, we consider the comparison to be legitimate, because in both systems a facetted nanocrystal with a high affinity for thiol groups dispersed in an apolar solvent is considered. For these simulations, the rigid aromatic molecules (i.e., BDT, BPE, BdMT) were mimicked by HdT molecules, where the torsional force constants along the carbon chain were increased by a factor of 10 compared to the flexible HdT molecules. In this manner, the energy level of the gauche conformation increases from 2 to 20 kT at room temperature, ensuring that the molecule will stay in the anti conformation (i.e., a rigid molecule). The conformational energy penalty for cross-linkage to the nanocrystal surface with both thiol groups is too large for the rigid HdT molecules. Hence, they attach with one thiol group to the nanocrystal surface and the (rigid) chains are oriented away from this surface (Figure 5b). On the other hand, a large fraction of the flexible HdT molecules (five out of six in Figure 5a) can form loops on the nanocrystal surface due to their conformational freedom, which is in qualitative agreement with our observations. A detailed description of the simulations can be found in the Supporting Information.

In the literature, there is a consensus that aromatic dithiols (and BdMT in particular) stand upright on a gold surface.[21−24] In contrast, HdT was reported to lie flat on gold substrates, and the formation of loops by HdT has been reported as well.[25,26] On the other hand, the upright orientation of HdT or octanedithiol molecules was also reported, and there is an extensive ongoing debate about the orientation of these flexible dithiols on gold substrates.[7,27,28] In addition, it should be mentioned that a recent theoretical paper showed that benzene-1,4-dithiol lies almost flat on a gold surface at low coverage, although only one thiol group is bound to the surface in that case.[29] The present results show that there is indeed a difference in orientation between flexible and rigid dithiols on a nanocrystal surface: the high fraction f of 0.34 for BPD as cross-linker suggests that rigid dithiols bind with only one thiol to the nanocrystal in an upright position, whereas flexible dithiols ($f \approx 0.08$) prefer to form loops and attach with both thiols to the surface.

Red-Shifts. Further support for the binding of the dithiols with both thiol groups on the surface of the QDs is obtained from the analysis of the red-shift of the absorption (and emission) spectra upon the addition of either dithiols (flexible or rigid) or monothiols. In a previous publication we reported on a red-shift of both the emission and absorption band of green-emitting QDs upon the addition of dithiol linker molecules.[11] The red-shift was strongly size-dependent and was observed to be much smaller for larger (red-emitting) QDs. To explain the size-dependent red-shift we presented a model in which the interaction between QDs was calculated from the wavefunction overlap between charge carriers in neighboring QDs. As the extension of the wavefunction outside the QD is higher in the stronger confinement regime, a larger coupling is expected for the smaller QDs, in agreement with the experimental results. To investigate the validity of this model, the optical properties of gQDs were studied after addition of monothiols. If the red-shift is indeed related to electronic coupling between cross-linked QDs, no red-shift is expected for this system, since no coupling occurs by the addition of monothiols. In a range of 1−4000 monothiols per QD, the shift in the first absorption peak was investigated for propanethiol (PT), hexanethiol (HT), nonanethiol (NT), benzenethiol (BT), and phenylethanethiol (PET), see Figure 6. The first absorption maximum of gQDs already shifts significantly in the range of 5−40 monothiols per QD, saturating at a level of 40 meV. The shift increases with increasing monothiol concentration and is independent of the type of monothiol used, indicating that it is an effect purely caused by the substitution of amine groups by the thiol groups. The reason for the decrease in absorption shift in the particular case of gQDs cross-linked by BT at high concentrations is unclear. The maximum shift of the first absorption peak of gQDs that were cross-linked by HdT was also 40 meV. Therefore, it can be concluded that the red-shift in absorption for gQD aggregates is not due to strong electronic coupling but is an effect of thiol groups attaching to the nanocrystal surface. The absence of a red-shift in the case of rigid cross-linkers is simply due to the low concentration of cross-linkers used in these experiments (linker/QD ratio up to 2:1).

In the range of 1−40 monothiols per QD, the red-shift depends approximately linearly on the molar thiol/QD ratio, i.e., the number of thiols attached to the nanocrystal surface. Importantly, Figure 6b shows that the red-shift of the first absorption peak increases faster as a function of the thiol/QD ratio when dithiols are used (HdT and NdT) as compared to monothiols (HT and NT). The slope of the red-shift as a function of the thiol concentration is about a factor of 2 steeper for the dithiols in comparison to the monothiols (see Figure 6b). These results from optical absorption measurements prove in a unique way that flexible cross-linkers attach with both thiol groups to the nanocrystal surface to form loops.

To study if the red-shift in the absorption spectrum after thiol substitution is dependent on the nanocrystal size and/or type, CdTe and CdSe QDs of different sizes were prepared. Figure 7 shows the absorption spectra of green-, yellow-, and red-emitting CdTe and CdSe QDs before and after the addition of an excess of HT (molar ratio thiol/QD > 25.000). For both CdTe and CdSe QDs, the smallest QDs (gQDs) show a significant red-shift of the first absorption maximum, whereas the larger QDs (yQDs and rQDs) show a small or no red-shift at all. The exciton emission peak of these samples all shifted in a similar way as the first absorption peak (not shown). The red-shift of rQDs at various monothiol concentrations is plotted in Figure 6a, which also shows that the red-shift is much smaller as compared to the gQDs (10 versus 40 meV). This apparent size-dependent red-shift of the (first) absorption and emission peak due to the attachment of thiols cannot be explained easily. Two tentative explanations for the size-dependent red-shift are given below.

In the first place, one might consider the replacement of amines by thiol groups at Cd-terminated facets on the nanocrystal surface as an expansion of the (electronic) size of the QD. In that case, the confinement of the charge carriers is smaller, leading to a smaller optical gap. Qualitatively, this could

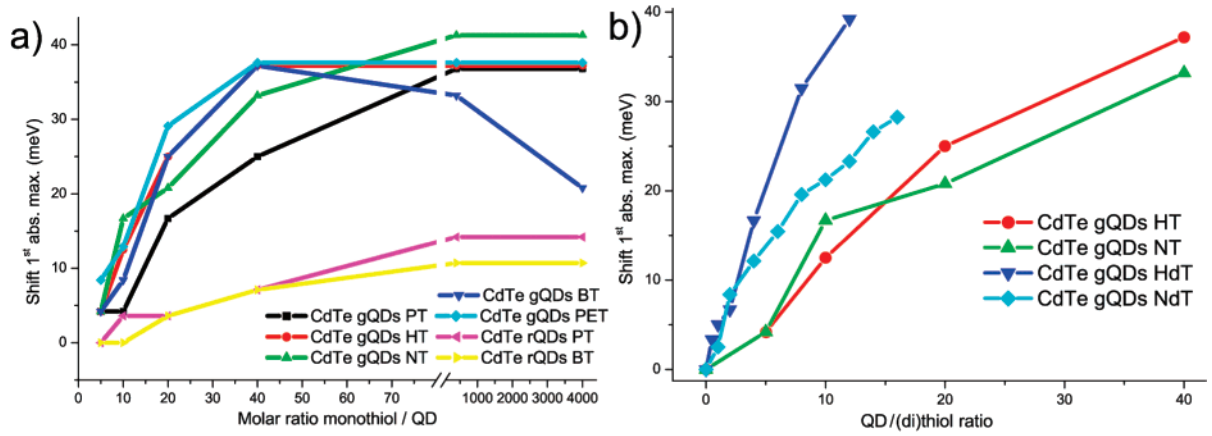

Figure 6. Red-shift of the first absorption maximum of green- and red-emitting AA-capped CdTe QDs (gQDs and rQDs), as a function of the thiol/QD ratio: (a) red-shift of gQDs and rQDs for five different monothiols; (b) comparison of the red-shift of gQDs after addition of monothiols (HT and NT) or dithiols (HdT and NdT).

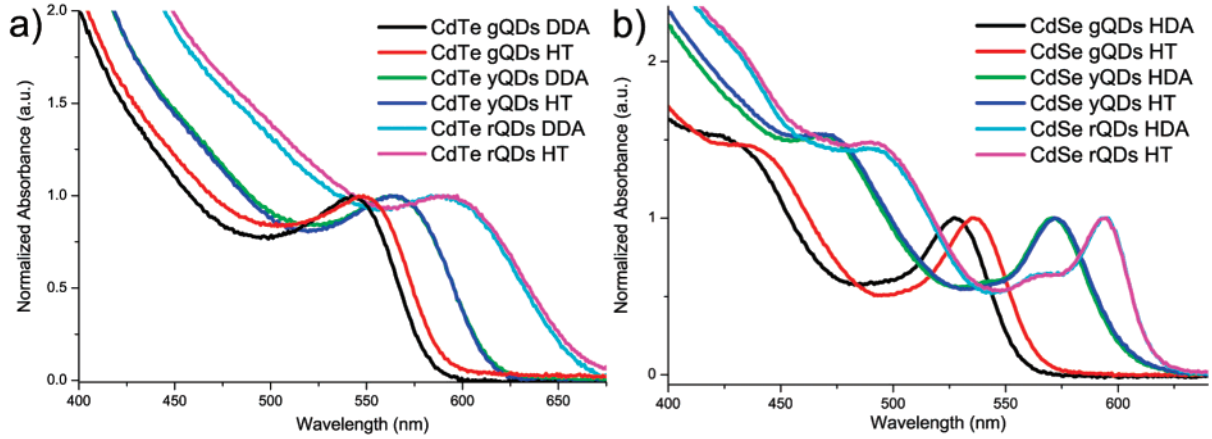

Figure 7. Normalized absorption spectra of green-, yellow-, and red-emitting CdTe (a) and CdSe (b) QDs, dispersed in toluene with their original capping (DDA or HDA), and after addition of an excess of hexanethiol (HT) (HT/QD > 25.000).

explain why the red-shift is larger for the smallest QDs, for which quantum confinement is the largest. According to the formula of Sapra and Sarma, relating the confinement energy to the size of a nanocrystal, we calculate that the band gap of the gQDs would decrease by 67 meV after the attachment of a monolayer of thiols.[30] For this calculation, a gQD diameter of 3.4 nm, a Cd−S bond length of 0.28 nm, and a 50% termination of the surface by Cd ions are assumed. Furthermore, it is hypothesized that a monolayer of thiol groups has a similar effect on the band gap as the addition of a monolayer of Te ions. It should be noted that a Cd surface passivated by thiol ligand bonds may not be regarded as an inorganic CdS shell, because the latter should result in an increase in the quantum yield of the CdSe QDs.[31] Instead, we observe a decrease in the quantum yield upon addition of thiols to the CdSe QDs, which was reported earlier and ascribed to hole-trapping by the thiol ligands.[32] A similar treatment for the rQDs (5.1 nm in diameter) in Figure 7a yields an expected decrease in band gap of 29 meV. From experiments, a maximum red-shift of 40 and 10 meV was observed for the gQDs and rQDs, respectively (Figure 6a). Second, both an experimental and theoretical paper have shown that the Cd−thiol bond is significantly stronger for smaller CdTe and CdSe nanocrystals compared to larger QDs.[33,34] It can be argued that a stronger Cd−thiol bond results in a larger influence of the thiol group on the electronic structure of the QD. This may be connected with the size-dependent red-shift that is observed upon the attachment of monothiols on the surface of CdSe and CdTe QDs (Figure 7).

Conclusions

In summary, we have investigated the cross-linking of CdTe QDs by dithiol linker molecules. The results (cryo-TEM and optical spectroscopy) show that rigid dithiol molecules such as BPD are more efficient cross-linkers than flexible dithiol molecules, such as HdT. Upon adding dithiol linker molecules, the emission spectra shift to longer wavelengths, the relative intensity of the defect emission increases, and the luminescence decay curves show a fast initial decay due to exciton energy transfer to QDs with a smaller band gap within the aggregate. These effects occur at much lower linker/QD ratios for the rigid linker molecules compared to the flexible dithiols. A quantitative analysis of the luminescence decay curves shows that the rigid dithiols cross-link the QDs at least 4 times more efficient than flexible cross-linkers. This is attributed to the formation of loops of the flexible dithiols on a QD surface by attaching with both thiol groups to the same QD, which is not possible for the rigid dithiols. Molecular simulations confirm the formation of loops by the flexible HdT on a nanocrystal with a strong affinity for thiol groups. Further experimental evidence for the formation of loops is obtained from the red-shift of the exciton emission band that is observed upon addition of both mono- and dithiols. The red-shift is induced by the exchange of amine capping molecules by thiols and not by electronic coupling as we previously reported. For the flexible dithiols the same shift is

observed as for monothiols at half the concentration, providing evidence that the dithiols bind with both thiol groups at the QD surface.

Acknowledgment. We thank Hans Meeldijk for taking all the TEM images. Financial support from the European Union network "FULLSPECTRUM" (SES6-CT-2003-502620) is gratefully acknowledged.

Supporting Information Available: Experimental details about cryo-TEM and the molecular simulations, cryo-TEM images, more decay curves, and the derivation of eq 1. This material is available free of charge via the Internet at http://pubs.acs.org.

References and Notes

(1) Oosterkamp, T. H.; Fujisawa, T.; van der Wiel, W. G.; Ishibashi, K.; Hijman, R. V.; Tarucha, S.; Kouwenhoven, L. P. *Nature* **1998**, *395*, 873.

(2) Stinaff, E. A.; Scheibner, M.; Bracker, A. S.; Ponomarev, I. V.; Korenev, V. L.; Ware, M. E.; Doty, M. F.; Reinecke, T. L.; Gammon, D. *Science* **2006**, *311*, 636.

(3) Bayer, M.; Hawrylak, P.; Hinzer, K.; Fafard, S.; Korkusinski, M.; Wasilewski, Z. R.; Stern, O.; Forchel, A. *Science* **2001**, *291*, 451.

(4) Shevchenko, E. V.; Talapin, D. V.; O'Brien, S.; Murray, C. B. *J. Am. Chem. Soc.* **2005**, *127*, 8741.

(5) Brousseau, L. C.; Novak, J. P.; Marinakos, S. M.; Feldheim, D. L. *Adv. Mater.* **1999**, *11*, 447.

(6) Dadosh, T.; Gordin, Y.; Krahne, R.; Khivrich, I.; Mahalu, D.; Frydman, V.; Sperling, J.; Yacoby, A.; Bar-Joseph, I. *Nature* **2005**, *436*, 1200.

(7) Schreiber, F. *Prog. Surf. Sci.* **2000**, *65*, 151.

(8) Reed, M. A.; Zhou, C.; Muller, C. J.; Burgin, T. P.; Tour, J. M. *Science* **1997**, *278*, 252.

(9) Nitzan, A.; Ratner, M. A. *Science* **2003**, *300*, 1384.

(10) Joachim, C.; Gimzewski, J. K.; Aviram, A. *Nature* **2000**, *408*, 541.

(11) Koole, R.; Liljeroth, P.; de Mello Donega, C.; Vanmaekelbergh, D.; Meijerink, A. *J. Am. Chem. Soc.* **2006**, *128*, 10436.

(12) Wuister, S. F.; van Driel, F.; Meijerink, A. *Phys. Chem. Chem. Phys.* **2003**, *5*, 1253.

(13) de Mello Donega, C.; Bode, M.; Meijerink, A. *Phys. Rev. B* **2006**, *74*, 085320.

(14) Yu, W. W.; Qu, L.; Guo, W.; Peng, X. *Chem. Mater.* **2003**, *15*, 2854.

(15) Crooker, S. A.; Hollingsworth, J. A.; Tretiak, S.; Klimov, V. I. *Phys. Rev. Lett.* **2002**, *89*, 186802.

(16) Achermann, M.; Petruska, M. A.; Crooker, S. A.; Klimov, V. I. *J. Phys. Chem. B* **2003**, *107*, 13782.

(17) Franzl, T.; Koktysh, D. S.; Klar, T. A.; Rogach, A. L.; Feldmann, J.; Gaponik, N. *Appl. Phys. Lett.* **2004**, *84*, 2904.

(18) Franzl, T.; Shavel, A.; Rogach, A. L.; Gaponik, N.; Klar, T. A.; Eychmuller, A.; Feldmann, J. *Small* **2005**, *1*, 392.

(19) Tachiya, M. *J. Chem. Phys.* **1982**, *76*, 340.

(20) Novak, J. P.; Feldheim, D. L. *J. Am. Chem. Soc.* **2000**, *122*, 3979.

(21) Pugmire, D. L.; Tarlov, M. J.; van Zee, R. D.; Naciri, J. *Langmuir* **2003**, *19*, 3720.

(22) Tour, J. M.; Jones, L.; Pearson, D. L.; Lamba, J. J. S.; Burgin, T. P.; Whitesides, G. M.; Allara, D. L.; Parikh, A. N.; Atre, S. V. *J. Am. Chem. Soc.* **1995**, *117*, 9529.

(23) Zareie, H. M.; McDonagh, A. M.; Edgar, J.; Ford, M. J.; Cortie, M. B.; Phillips, M. R. *Chem. Mater.* **2006**, *18*, 2376.

(24) Hong, S.; Reifenberger, R.; Tian, W.; Datta, S.; Henderson, J. I.; Kubiak, C. P. *Superlattices Microstruct.* **2000**, *28*, 289.

(25) Leung, T. Y. B.; Gerstenberg, M. C.; Lavrich, D. J.; Scoles, G.; Schreiber, F.; Poirier, G. E. *Langmuir* **2000**, *16*, 549.

(26) Bain, C. D.; Troughton, E. B.; Tao, Y. T.; Evall, J.; Whitesides, G. M.; Nuzzo, R. G. *J. Am. Chem. Soc.* **1989**, *111*, 321.

(27) Aliganga, A. K. A.; Duwez, A. S.; Mittler, S. *Org. Electron.* **2006**, *7*, 337.

(28) Yang, Y. C.; Lee, Y. L.; Yang, L. Y. O.; Yau, S. L. *Langmuir* **2006**, *22*, 5189.

(29) Pontes, R. B.; Novaes, F. D.; Fazzio, A.; daSilva, A. J. R. *J. Am. Chem. Soc.* **2006**, *128*, 8996.

(30) Sapra, S.; Sarma, D. D. *Phys. Rev. B* **2004**, *69*, 125304.

(31) Peng, X. G.; Schlamp, M. C.; Kadavanich, A. V.; Alivisatos, A. P. *J. Am. Chem. Soc.* **1997**, *119*, 7019.

(32) Wuister, S. F.; Donega, C. D.; Meijerink, A. *J. Phys. Chem. B* **2004**, *108*, 17393.

(33) Schrier, J.; Wang, L. W. *J. Phys. Chem. B* **2006**, *110*, 11982.

(34) Aldana, J.; Lavelle, N.; Wang, Y. J.; Peng, X. G. *J. Am. Chem. Soc.* **2005**, *127*, 2496.